

Optical external efficiency calculation for mid-infrared quantum cascade laser

ABDELOUAHAB HAMADOU

Département de Génie Mécanique, Université Abdelhamid Ibn Badis de Mostaganem, Algeria;
e-mail: abd_hamado@yahoo.fr

In this paper, we present a simple method for calculation of optical external efficiency of mid-infrared quantum cascade laser. The approach is based on the three-level rate equations describing the variation of the electron number in the excited states and the photon number present within the cavity. We have obtained a simple analytical formula for the optical external efficiency. The effects of cavity lengths and current injection are taken into account. It has been found that the optical external efficiency becomes more important at high current injection and at lower cavity lengths.

Keywords: quantum cascade laser, rate equations, output power, optical external efficiency.

1. Introduction

Quantum cascade (QC) laser [1] is a unipolar semiconductor device that utilizes intersubband transitions in quantum wells. In these lasers, the wavelength is not controlled by the material bandgap but by the choice of well and barrier layer thickness and by tailoring the optical matrix elements and the relaxation times. Up to now, a number of authors have proposed various operating schemes for mid-infrared QC laser. Among the notable designs, the following can be mentioned: the three quantum wells active region scheme [2–5], the superlattice active region design [6–8], the two phonons active region one [9], and the bound to continuum design [10–13]. Optical performance on QC laser depends of an important parameter, namely the optical external efficiency. This efficiency depends on the laser cavity length and on the current injection. In this paper, we calculate the optical external efficiency η_{ext} for the mid-infrared QC laser reported by PAGE *et al.* [3], using a rate equation model.

2. Theory

2.1. Rate equation model

The simplified rate equations describing the variation of the numbers of electrons in the excited states N_3 and N_2 and the number of photons N_{ph} in the cavity can be written as [14, 15]:

$$\frac{dN_3}{dt} = \frac{I}{e} - \frac{N_3}{\tau_3} - \Gamma \frac{c' \sigma_{32}}{V} (N_3 - N_2) N_{\text{ph}} \quad (1a)$$

$$\frac{dN_2}{dt} = \frac{N_3}{\tau_{32}} - \frac{N_2}{\tau_{21}} + \Gamma \frac{c' \sigma_{32}}{V} (N_3 - N_2) N_{\text{ph}} \quad (1b)$$

$$\frac{dN_{\text{ph}}}{dt} = N\Gamma \frac{c' \sigma_{32}}{V} (N_3 - N_2) N_{\text{ph}} - \frac{N_{\text{ph}}}{\tau_p} \quad (1c)$$

where spontaneous emission has been neglected and a single laser mode has been assumed.

In the above equations, I denotes the injected current tunnelling into the upper laser level and e is the electronic charge, while Γ and σ_{32} are the mode confinement factor for the cavity and the stimulated emission cross-section between the upper and lower laser levels. In addition, in the above equations we introduced the total number of cascaded gain stages N and the velocity of the light in medium $c' = c/n_{\text{eff}}$, where c and n_{eff} are the speed of light in vacuum and the effective refractive index of the cavity. To complete the picture we take into consideration the volume of the cavity denoted by V and given by $V = NL_p WL$, where L_p is the length of a single stage while W and L are the width and the length of the cavity, respectively. The three nonradiative scattering times, denoted by τ_{32} , τ_{31} , and τ_{21} , are calculated accounting only for longitudinal optical phonon emission, which is assumed to be by far the dominant scattering mechanism [16]. We also define the lifetime of the upper laser level τ_3 given by $\tau_3^{-1} = \tau_{32}^{-1} + \tau_{31}^{-1}$. The photon lifetime τ_p is given by [17]:

$$\frac{1}{\tau_p} = c' \left(\alpha_w - \frac{1}{L} \ln \sqrt{R_1 R_2} \right) \quad (2)$$

where R_1 and R_2 are the output couplings at facets 1 and 2, and α_w denotes the waveguide losses of the cavity. The latter is caused in QC laser by the free carrier absorption in the doped semiconductor regions and the metallic contact layers, the scattering loss out of the optical waveguide, and some loss in the passive portions of the guide and in the cladding.

In order to determine the intensity inside the active medium of the QC laser, we calculate the population inversion between excited states 3 and 2. The system of

Equations (1) can be solved for steady-state conditions, yielding after a somewhat lengthy calculation the following expression for population inversion

$$\Delta N = \frac{\frac{I}{e} \tau_3 \left(1 - \frac{\tau_{21}}{\tau_{32}}\right)}{1 + \frac{N_{\text{ph}}}{N_{\text{ph, sat}}}} \quad (3)$$

where $N_{\text{ph, sat}}$ is the saturation photon number, given by

$$N_{\text{ph, sat}} = \frac{V}{\tau_{\text{sat}} \Gamma c' \sigma_{32}} \quad (4)$$

In Equation (4), τ_{sat} is the saturation time constant defined as

$$\tau_{\text{sat}} = \tau_3 \left(1 + \frac{\tau_{21}}{\tau_{31}}\right) \quad (5)$$

The rate equation (1c), with the help of Eqs. (2), (3) and (4), leads to the steady-state photon number N_{ph} as a function of current injection:

$$N_{\text{ph}} = N_{\text{ph, sat}} \left(\frac{I}{I_{\text{th}}} - 1\right) \quad (6)$$

where I_{th} denotes the threshold current, which we define by equating the modal gain and the losses.

At threshold, we have

$$N \frac{\Gamma \sigma_{32}}{V} \Delta N_{\text{th}} = \alpha_w - \frac{1}{L} \ln \sqrt{R_1 R_2} \quad (7)$$

where the population inversion at threshold ΔN_{th} is obtained from Eq. (3) by setting N_{ph} to zero and replacing I by I_{th} . After easy algebra we get the following expression for I_{th} :

$$I_{\text{th}} = \frac{e W L_p}{\Gamma \sigma_{32}} \frac{1}{\tau_3 \left(1 - \frac{\tau_{21}}{\tau_{32}}\right)} \left(\alpha_w L - \ln \sqrt{R_1 R_2}\right) \quad (8)$$

As we can see from Eq. (8) the output coupling at facets 1 and 2, the waveguide losses of the cavity, the stimulated emission cross-section, the cavity length, and

the confinement factor are the parameters determining the threshold current in QC laser. In addition, the structural parameter of the QC laser (layer widths and composition) affect also the nonradiative scattering times, and thus the threshold current [18, 19].

Considering the fact that the intensity inside the active medium is doubled, the intensity of light traveling inside the cavity of QC laser, calculated by using Eq. (6) and taking into account the relationship between intensity in units of W/cm² and photon number in the cavity $2I_0 = I_0^+ + I_0^- = c' \hbar \omega N_{\text{ph}}/V$ [17], is given by:

$$I_0 = \frac{I_{0, \text{sat}}}{2} \left(\frac{I}{I_{\text{th}}} - 1 \right) \quad (9)$$

where I_0^+ and I_0^- are, respectively, the forward and backward traveling beam in the cavity, $\hbar \omega$ is the energy of emitted photon, and $I_{0, \text{sat}} = c' \hbar \omega N_{\text{ph, sat}}/V$ is the saturation intensity.

2.2. Output power and optical external efficiency

The system of Eqs. (1) describing the amplification of the QC laser light inside the active medium is now used to derive the output power P_{out} and the optical external efficiency η_{ext} . The output power P_{out} is related to light intensity by $P_{\text{out}} = A(1 - R)I_0$ where $R = R_1 = R_2$ and $A = NWL_p$ is the cross-sectional area of the QC laser. Using Eq. (9), one gets

$$P_{\text{out}} = NWL_p(1 - R) \frac{I_{0, \text{sat}}}{2} \left(\frac{I}{I_{\text{th}}} - 1 \right) \quad (10)$$

The power transferred into the upper laser level P_{UL} is attained when the waveguide losses of the cavity are zero and the output coupling R approaches 100% (*i.e.*, $R \rightarrow 1$). Inserting Eq. (8) into Eq. (10), and using the approximation $(1 - R) \approx |\ln(R)|$, the following expression for P_{UL} is obtained:

$$P_{\text{UL}} = N \frac{I_{0, \text{sat}}}{2} \frac{\Gamma \sigma_{32}}{e} \tau_3 \left(1 - \frac{\tau_{21}}{\tau_{32}} \right) I \quad (11)$$

We see that the output power will generally be lower than this maximum value. We now wish to derive a general expression for the optical external efficiency η_{ext} which is an important parameter to characterise the optical performance of a QC laser. This quantity is defined as the ratio of the output power emitted by stimulated emission and the power transferred into the upper laser level:

$$\eta_{\text{ext}} = \frac{P_{\text{out}}}{P_{\text{UL}}} \quad (12)$$

Using Eqs. (10) and (11) together with Eq. (8), we readily obtain the important optical external efficiency parameter

$$\eta_{\text{ext}} = (1 - R) \left(\frac{1}{\alpha_w L - \ln(R)} - \frac{eWL_p}{\Gamma\sigma_{32}\tau_3 \left(1 - \frac{\tau_{21}}{\tau_{32}}\right) I} \right) \quad (13)$$

As we can see from Eq. (13) the optical external efficiency depends on the material parameters of QC laser and can be controlled either by the cavity length L or by the current injection I . For the case of very high current injection, we find that the value for η_{ext} given by Eq. (13) is well approximated by the relation

$$\eta_{\text{ext}} \approx \frac{1 - R}{\alpha_w L - \ln(R)} \quad (14)$$

This equation indicates that the optical external efficiency is mostly controlled by two important parameters, namely the cavity length and waveguide losses. A similar result was obtained by FAIST [20].

3. Numerical results and discussion

In the following discussion we study the effects of cavity length and current injection on the output power and the optical external efficiency for the structure of QC laser described in Ref. [3]. We use in our calculation the parameters taken from Refs. [3, 21]: number of cascaded gain stages $N = 48$, waveguide losses of the cavity $\alpha_w = 20 \text{ cm}^{-1}$, nonradiative scattering times $\tau_{32} = 2.1 \text{ ps}$, $\tau_{21} = 0.3 \text{ ps}$, lifetime of the upper laser level $\tau_3 = 1.4 \text{ ps}$, width of the cavity $W = 34 \text{ }\mu\text{m}$, length of a single stage of the cascade laser structure $L_p = 45 \text{ nm}$, mode confinement factor for the cavity $\Gamma = 0.32$, output coupling $R = 0.29$, and the calculated parameters from Ref. [15]: saturation photon number $N_{\text{ph, sat}} = 9.16 \times 10^8$ and stimulated emission cross-section $\sigma_{32} = 1.8 \times 10^{-14} \text{ cm}^2$.

In order to illustrate the influence of the cavity on the optical performance of QC laser we plot in Fig. 1 the output power as a function of current injection for different cavity lengths $L = 0.1 \text{ cm}$ (solid line), 0.2 cm (dashed line), 0.3 cm (dotted line), and 0.4 cm (dot-dashed line). The curve marked by ‘‘upper laser level’’ is the power transferred into the upper laser level. The output power increases linearly with current injection up to the threshold and the slope efficiency becomes steeper as the cavity length is increased. The output power cannot exceed the power P_{UL} that is available in the cavity.

Figure 2 shows the effect of the cavity length and the current injection on the optical performance of the QC laser. The figure depicts contour lines of optical external efficiency η_{ext} as a function of the cavity length and the current injection. It has been

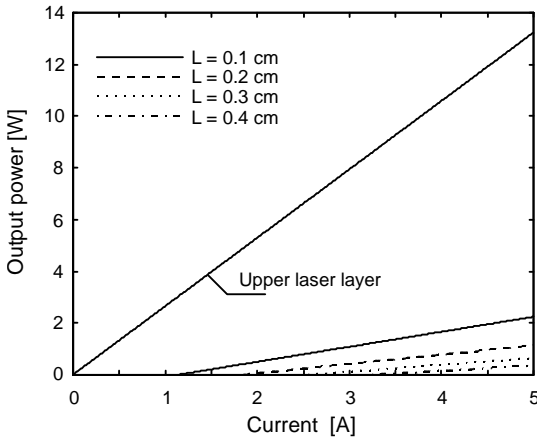


Fig. 1. Calculated output power as a function of current injection for different cavity lengths. The solid, dashed, dotted and dot-dashed curves stand for $L = 0.1, 0.2, 0.3$ and 0.4 cm, respectively. The curve marked by “upper laser level” is the power transferred into the upper laser level.

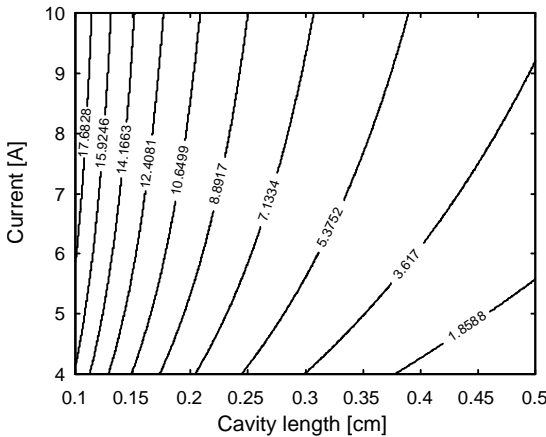


Fig. 2. Calculated contour plot of the optical external efficiency η_{ext} [%] as a function of the cavity length and current injection.

found that the optical external efficiency depends strongly on the cavity length and the current injection. The optimal choice of $L < 0.15$ cm and $I > 5$ A results in the greatest value of $\eta_{ext} > 10\%$.

The optical external efficiency calculated from Eq. (13) for four cavity lengths $L = 0.1$ cm (solid line), 0.2 cm (dashed line), 0.3 cm (dotted line), and 0.4 cm (dot-dashed line) is plotted in Fig. 3. As can be seen, the optical external efficiency first increases rapidly with the current injection I and then saturates for the highest values of I . This figure also shows that, when the cavity is lengthened, the threshold current is significantly increased and the maximum optical external efficiency at high current injection is reduced.

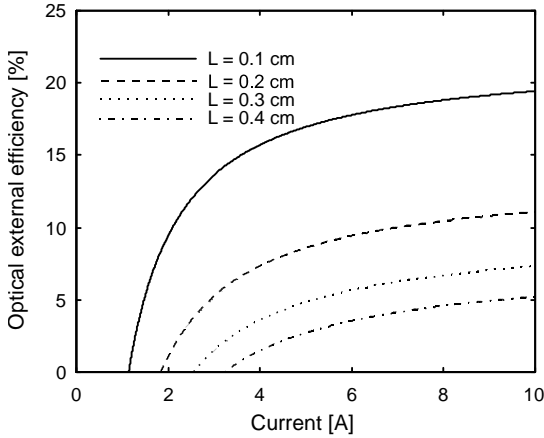


Fig. 3. Dependence of optical external efficiency versus current injection for different cavity lengths. The solid, dashed, dotted and dot-dashed curves stand for $L = 0.1, 0.2, 0.3$ and 0.4 cm, respectively.

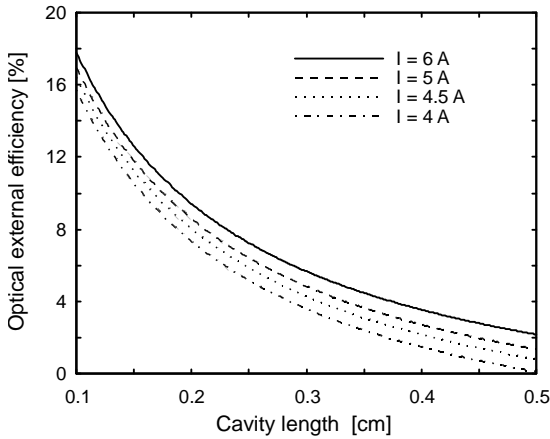


Fig. 4. Dependence of optical external efficiency versus cavity length for different current injections. The solid, dashed, dotted and dot-dashed curves stand for $I = 6, 5, 4.5$ and 4 A, respectively.

In Figure 4, the optical external efficiency is plotted as a function of the cavity length for four values of current injection $I = 6$ A (solid line), 5 A (dashed line), 4.5 A (dotted line), and 4 A (dot-dashed line). We observe that the optical external efficiency decreases when the cavity is lengthened. It becomes lower than 2% at $I \leq 6$ A for cavity larger than 0.5 cm.

4. Conclusions

In summary, we have developed a new method to obtain the optical external efficiency of mid-infrared QC laser, using a simple rate equation model. In particular, a simple analytical formula for the optical external efficiency was derived. It has been shown

that the output power accounts for less than 18% of the power transferred into the upper laser level and varies strongly with cavity length. The results should be generally applicable to a wide class of mid-infrared QC lasers.

Acknowledgments – The author wishes to acknowledge the help of J.-L. Thobel, from Institut d'Electronique, de Microélectronique et de Nanotechnologie (IEMN), UMR 8520, Université des Sciences et Technologies de Lille1, France.

References

- [1] FAIST J., CAPASSO F., SIVCO D.L., SIRTORI C., HUTCHINSON A.L., CHO A.Y., *Quantum cascade laser*, *Science* **264**(5158), 1994, pp. 553–556.
- [2] SIRTORI C., KRUCK P., BARBIERI S., COLLOT P., NAGLE J., BECK M., FAIST J., OESTERLE U., *GaAs/Al_xGa_{1-x}As quantum cascade lasers*, *Applied Physics Letters* **73**(24), 1998, pp. 3486–3488.
- [3] PAGE H., BECKER C., ROBERTSON A., GLASTRE G., ORTIZ V., SIRTORI C., *300 K operation of a GaAs-based quantum-cascade laser at $\lambda \approx 9 \mu\text{m}$* , *Applied Physics Letters* **78**(22), 2001, pp. 3529–3531.
- [4] CARDER D.A., WILSON L.R., GREEN R.P., COCKBURN J.W., HOPKINSON M., STEER M.J., AIREY R., HILL G., *Room-temperature operation of an InAs–GaAs–AlAs quantum-cascade laser*, *Applied Physics Letters* **82**(20), 2003, pp. 3409–3411.
- [5] NG W.H., ZIBIK E.A., SOULBY M.R., WILSON L.R., COCKBURN J.W., LIU H.Y., STEER M.J., HOPKINSON M., *Broadband quantum cascade laser emitting from 7.7 to 8.4 μm operating up to 340 K*, *Journal of Applied Physics* **101**(4), 2007, p. 046103.
- [6] SCAMARCIO G., CAPASSO F., SIRTORI C., FAIST J., HUTCHINSON A.L., SIVCO D.L., CHO A.Y., *High-power infrared (8-micrometer wavelength) superlattice lasers*, *Science* **276**(5313), 1997, pp. 773–776.
- [7] TREDICUCCI A., CAPASSO F., GMACHL C., SIVCO D.L., HUTCHINSON A.L., CHO A.Y., FAIST J., SCAMARCIO G., *High-power inter-miniband lasing in intrinsic superlattices*, *Applied Physics Letters* **72**(19), 1998, pp. 2388–2390.
- [8] ANDERS S., SCHRENK W., GORNIK E., STRASSER G., *Room-temperature emission of GaAs/AlGaAs superlattice quantum-cascade lasers at 12.6 μm* , *Applied Physics Letters* **80**(11), 2002, pp. 1864–1866.
- [9] HOFSTETTER D., BECK M., AELLEN T., FAIST J., *High-temperature operation of distributed feedback quantum-cascade lasers at 5.3 μm* , *Applied Physics Letters* **78**(4), 2001, pp. 396–398.
- [10] FAIST J., BECK M., AELLEN T., GINI E., *Quantum-cascade lasers based on a bound-to-continuum transition*, *Applied Physics Letters* **78**(2), 2001, pp. 147–149.
- [11] WALTHER C., SCALARI G., FAIST J., BEERE H., RITCHIE D., *Low frequency terahertz quantum cascade laser operating from 1.6 to 1.8 THz*, *Applied Physics Letters* **89**(23), 2006, p. 231121.
- [12] DEVENSON J., BARATE D., CATHABARD O., TEISSIER R., BARANOV A.N., *Very short wavelength ($\lambda = 3.1\text{--}3.3 \mu\text{m}$) quantum cascade lasers*, *Applied Physics Letters* **89**(19), 2006, p. 191115.
- [13] SCALARI G., SIRIGU L., TERAZZI R., WALTHER C., AMANTI M.I., GIOVANNINI M., HOYLER N., FAIST J., SADOWSKI M.L., BEERE H., RITCHIE D., DUNBAR L.A., HOUDRÉ R., *Multi-wavelength operation and vertical emission in THz quantum-cascade lasers*, *Journal of Applied Physics* **101**(8), 2007, p. 081726.
- [14] HAMADOU A., THOBEL J.-L., LAMARI S., *Modelling of temperature effects on the characteristics of mid-infrared quantum cascade lasers*, *Optics Communications* **281**(21), 2008, pp. 5385–5388.
- [15] HAMADOU A., LAMARI S., THOBEL J.-L., *Dynamic modeling of a midinfrared quantum cascade laser*, *Journal of Applied Physics* **105**(9), 2009, p. 093116.

- [16] FERREIRA R., BASTARD G., *Evaluation of some scattering times for electrons in unbiased and biased single- and multiple-quantum-well structures*, Physical Review B **40**(2), 1989, pp. 1074–1086.
- [17] YARIV A., *Quantum Electronics*, 3rd Edition, John Wiley and Sons, New York, 1988.
- [18] DANIČIĆ A., RADOVANOVIĆ J., MILANOVIĆ V., INDJIN D., IKONIĆ Z., *Optimization and magnetic-field tunability of quantum cascade laser for applications in trace gas detection and monitoring*, Journal of Physics D: Applied Physics **43**(4), 2010, p. 045101.
- [19] RADOVANOVIĆ J., MIRČETIĆ A., MILANOVIĆ V., IKONIĆ Z., INDJIN D., HARRISON P., KELSALL R.W., *Influence of the active region design on output characteristics of GaAs/AlGaAs quantum cascade lasers in a strong magnetic field*, Semiconductor Science and Technology **21**(3), 2006, pp. 215–220.
- [20] FAIST J., *Wallplug efficiency of quantum cascade lasers: Critical parameters and fundamental limits*, Applied Physics Letters **90**(25), 2007, p. 253512.
- [21] HOFLING S., KALLWEIT R., SEUFERT J., KOETH J., REITHMAIER J.P., FORCHEL A., *Reduction of the threshold current density of GaAs/AlGaAs quantum cascade lasers by optimized injector doping and growth conditions*, Journal of Crystal Growth **278**(1–4), 2005, pp. 775–779.

*Received October 5, 2010
in revised form January 30, 2011*